The Late Eocene-Early Miocene unconformities of the NW Indian Intraplate basins and Himalayan foreland: a record of tectonics or mantle dynamics?

Yani Najman[1*] Stuart D. Burley[2&3], Alex Copley[4], Michael J. Kelly[5], Kaushal Pander[5], and Premanand Mishra[5]

[1]Lancaster Environment Centre, Lancaster University, Lancaster, Lancashire, LA1 4YQ, UK
[2]Department of Earth Sciences, Keele University, Staffordshire ST5 5BG
and
[3]Orient Petroleum Ltd., 16, Upper Woburn Place, London WC1H 0AF
[4]COMET, Bullard Labs, Department of Earth Sciences, University of Cambridge, Cambridge, Cambridgeshire, CB3 0EZ, UK
[5]Cairn Oil and Gas, Vedanta Ltd, 3rd Floor, DLF Atria Building, DLF Phase II, Jacaranda Marg, DLF City, Gurgaon, 122 002, Haryana, India

* Corresponding author: Yani Najman (email: y.najman@lancs.ac.uk)

Key Points:

- The Late Eocene-Early Miocene unconformity of the NW Indian plate Intraplate basins is unrelated to Himalayan-induced compression or flexure.
- The unconformities of the NW Indian plate Intraplate basins and the Himalayan peripheral foreland basin are approximately coeval.
- A common mechanism is proposed for the foreland and intraplate basin unconformities related to mantle circulation.

Abstract

A well-developed Late Eocene to Miocene unconformity, termed the Base Miocene Unconformity (BMU), is found throughout the intraplate basins of north-western India, and has previously been ascribed to Himalayan tectonics. This hypothesis is investigated by first describing the nature and age of the BMU in the northwest Indian intraplate basins, and then reconstructing the location of the BMU relative to the Himalayan deformation front at the time it formed. We suggest that formation of the BMU in western India cannot be related to Himalayan tectonic processes associated with plate loading and flexure unless the Indian plate had an elastic thickness of >125 km, which is highly unlikely. Furthermore, the resumption of deposition post-unconformity rules out inversion due to compression associated with India-Asia convergence as a cause, as these compressive forces are still present. We note the coeval nature of the unconformity in the NW Indian plate intraplate basins and the Himalayan peripheral foreland basin. If the unconformities of the Himalayan peripheral foreland basin and the NW Indian intraplate basins formed by a common process, uplift due to circulation in the mantle is the only possible regional-scale mechanism. Such circulation could be the result of the intrinsically time-dependent high-Rayleigh number convection in the mantle, which has resulted in well-documented unconformities elsewhere, or be the result of subducting slab break-off beneath the Himalaya.

1. Introduction

The far field effects of continental collisions extend beyond the immediate realm of the orogen they create [*Cunningham*, 2005; *Otto*, 1997; *Replumaz and Tapponnier*, 2003]. At least two processes may cause regional stress changes associated with such collisions, that are expressed as folds, faulting and regional unconformities. Firstly, compressional stresses are laterally propagated for long distances into the foreland, for example as is documented in the western interior of the US and the Alpine orogen [e.g. *Dezes et al.*, 2004; *Dickinson and Snyder*, 1978]. Secondly, flexure of the previously-subducting plate occurs in the foreland due to loading by the mountain range and the under-thrusting slab [e.g *DeCelles et al.*, 1998; *Lyon-Caen and Molnar*, 1985]. To interpret the forces driving the creation of geological structures in the foreland of mountain ranges therefore requires distinguishing between flexural and far-field compressive effects, as well as separating these from deformation relating to sub-plate processes such as mantle convection and slab break-off.

In the case of the India-Asia collision, the Indian plate is under ~N-S compressive stress due to the forces arising from the central Indian Ocean mid-ocean ridge and the Tibetan Plateau [*Coblentz et al.*, 1995; *Copley et al.*, 2010]. The resulting deformation has been documented in a number of places, and takes the form of kilometre-scale reactivations of pre-existing faults [e.g. *Copley et al.*, 2014; *Müller et al.*, 2015], thrust-faulting earthquakes [e.g. *Craig et al.*, 2011], and folding and reverse faulting in the central Indian Ocean [e.g. *Krishna et al.*, 2009]. Flexure of the Indian plate has resulted in the development of the Himalayan foreland basin ahead of the southward migrating Himalayan thrust front, with a peripheral forebulge probably present to the south of this [*Bilham et al.*, 2003]. Migration of the forebulge either away from, or towards, the mountain range due to redistribution of the load, and the motion of the Indian plate (relative to the Himalayan range-front) through this region, are commonly proposed as the cause of the widespread ~Late Eocene to Early Miocene unconformity recorded throughout the peripheral foreland basin rocks now incorporated into the Sub-Himalayan thrust belt [*Bera et al.*, 2010; *DeCelles et al.*, 1998; *DeCelles et al.*, 2004; *Irfan et al.*, 2005; *Najman and Garzanti*, 2000; *Najman et al.*, 2005]. By contrast, Clift and VanLaningham [2010] suggest that redistribution of the load due to climatically-induced increased erosion of the orogen resulted in flexural unloading, unflexing of the Indian plate and consequential basin uplift and formation of the late

Eocene to early Miocene foreland basin unconformity. Mantle dynamics, including the break-off of subducting slabs, and the presence of hot thermal anomalies due to mantle upwelling, are additional suggested causes [e.g. *Husson et al.*, 2014; *Maheo et al.*, 2002].

The Barmer Basin is an inverted failed rift basin of Paleogene age [*Naidu et al.*, 2017], with its northern end situated ~800 km south of the Himalayan front and 400 km east of the Kirthar Mountains of central Pakistan (see Figures 1 and 2). *Compton* [2009], *Dolson et al.* [2015] and *Bladon et al.* [2015a] suggested that India-Asia collisional tectonics resulted in post-rift compressional features in the basin, including uplift of cross-rift basement ridges, inversion of the northern part of the basin (which has removed >1 km of sediment), and the major Late Eocene to Lower Miocene unconformity, termed the Base Miocene Unconformity (BMU). *Compton* [2009] correlated the BMU into the Jaisalmer / Middle Indus Basin, considered to be a Retreating Foreland Basin by DeCelles [2012]. The BMU is also traceable through a number of other basins distal to the Himalaya, including the Cambay, Kutch, Bombay and Indus basins, up to 1400 kms south of the Himalayan front, with decreasing intensity southwards (Figures 1 and 2). We term these basins the NW Indian intraplate basins. The purpose of this paper is to describe the nature and extent of the BMU in the NW Indian intraplate basins distal to the Himalaya, and to consider mechanisms for its formation in view of the previously proposed Himalayan influence. The description focusses on that part of the unconformity preserved in the Barmer Basin, Rajasthan, as a type example of the unconformity in the NW Indian intraplate basins, from where we interpret a wealth of sub-surface data made available by Cairn India.

2. Geological background; The NW Indian intraplate basins.

The BMU is documented and regionally mapped in the Barmer, Cambay, Kutch, [*Chowdhary*, 1975; *Chowdhary and Singh*, 1978; *Kundal et al.*, 2005] and Bombay (Mumbai) basins [*Basu et* *al.*, 1982; *Mehrotra et al.*, 2010; *M Mohan*, 1995; *Wandrey*, 2004] as an erosional event of generally decreasing erosional depth southwards (Figure 1, panels 5-7). In subsurface datasets it is recognised as a regional seismically correlatable reflection event (Figure 3). An equivalent unconformity is recognised in the onshore Jaisalmer Basin (Figure 1, panel 4); [*Quadri and Shuaib*, 1986; *Wandrey et al.*, 2004]. The offshore Indus Basin (Figure 2) also records Early Miocene erosional events [*Carmichael et al.*, 2009; *Clift et al.*, 2001; *Quadri and Shuaib*, 1986].

There are other less pronounced unconformities throughout the Paleogene and Miocene successions in the NW Indian intraplate basins [e.g. *Chowdhary*, 2004; *Mehrotra et al.*, 2010]. To the north, many of these are progressively eroded out by the BMU and merge onto the BMU surface, the erosional depth of which increases northwards. In the Sanchor and Cambay basins, the BMU erodes out progressively less of the Eocene and Oligocene successions until in depocentres of the southern Cambay Basin and the Bombay Offshore Basin almost complete Oligocene and Eocene successions are present (see Figure 1).

Local tectonics give rise to considerable variation in the architecture of the unconformities. For example, in the Cambay Basin the extent and intensity of these unconformities varies across rotated fault blocks in the basement. These are long-lived, fault bounded basement highs which in some cases include tilted Mesozoic sedimentary rocks [*Chowdhary and Singh*, 1978; *Mathuria et al.*, 2011; *R Mohan et al.*, 2008; *Sahoo and Choudhuri*, 2011] onto which the oldest Miocene sediments on-lap [*Dolson et al.*, 2015; *Kaila et al.*, 1990; *Mathuria et al.*, 2011; *Valdiya*, 1976]. Similarly, in the Bombay Offshore Basin, the depth of erosion is greatest across the larger fault blocks, such as the Bombay High [*Bhandari and Jain*, 1984; *Wandrey*, 2004]. Some structures in which the BMU is pronounced are associated with recent block uplift and inversion [*Huggett et al.*, 2015; *Pangtey*, 1996; *Sanyal et al.*, 2012] complicating the interpretation of erosional history. However, in general (Figure 1), the Jagadia Formation is regionally present across >600 km as the basal (oldest) continental Miocene sequence above the BMU in the Cambay and Barmer basins [*Dolson et al.*, 2015; *Kundal et al.*, 2005; *Naidu et al.*, 2017].

3. The Barmer Basin, Rajasthan; the BMU in a NW Indian Intraplate Basin.

In order to document the BMU in detail, in a region distal to the Himalayan front, the Barmer Basin has been studied because of its excellent seismic and exploration well coverage available from Cairn India. Seismic data covers almost 85% of the Barmer Basin, and more than 300 exploration wells have been drilled in the basin. Approximately 3000 line-km of vibroseis 2D seismic were acquired by Cairn India between 1995 and 2000, whilst several generations of 3D seismic data were joined into a mega-merged volume in 2013 and together cover ~6,200 km^2 of the basin, providing excellent seismic coverage for regional mapping.

The BMU and its enclosing stratigraphy are not cored anywhere in the Barmer Basin. However, in the >300 wells drilled in the basin cuttings samples were taken every 2 m and their lithology described, whilst a comprehensive suite of wireline logs was run in each well that included gamma-ray (GR), neutron-density, resistivity and sonic logs. These data in 38 key reference wells, along with biostratigraphic, apatite fission track and vitrinite reflectance data, form the basis of the descriptions provided below.

3.1 Basin Setting

The Barmer Basin, and its extension as the Sanchor sub-basin to the south (Figures 2 and 3), is a Cenozoic failed continental rift. The basin is the linear northward extension of the Cambay Basin within the West Indian Rift System, which extends for another 800 km southwards into the

Mumbai/Bombay Offshore Basin [*Biswas*, 1987; *Calvès et al.*, 2011; *Wandrey et al.*, 2004]. The Barmer Basin is separated from the Cambay Basin to the south by the SW-NE aligned Deodar Ridge / Mehsana High which are fault-bounded basement horsts of the Proterozoic Delhi Fold Belt [*Bhandari and Chowdhary*, 1975; *Kaila et al.*, 1990]. The Barmer Basin is separated from the Jaisalmer Basin to the north by the Devikot High [*Siddiquie*, 1963], a long-lived, basement structure with a thin Mesozoic sequence preserved across the top of the high. Gravity modelling indicates a depth to the Moho of 25-40 km across the Barmer Basin, consistent with regional studies of the crustal thickness of the Indian plate [*Kaila et al.*, 1990; *Singh et al.*, 2015].

3.2 Cenozoic Basin Stratigraphy

The Barmer Basin preserves a thick Neoproterozoic to Miocene stratigraphy overlain by Quaternary deposits [*Dhir and Singhvi*, 2012]. The full stratigraphy of the basin is detailed in *Compton* [2009], *Bladon et al.* [2015b] and *Dolson et al.* [2015] and summarised below to provide context for the Cenozoic sediments and their relationships to the BMU.

At least 6 km of Jurassic to Recent deposits overly the Neoproterozoic basement [*Sharma*, 2007]. Mesozoic successions within the basin which precede the Cenozoic rifting comprise fluvial Lower Jurassic Lathi Formation and fluvio-lacustrine Lower Cretaceous Ghaggar-Hakra Formations. Palaeocene-Early Eocene syn-rift deposits within the Barmer Basin are dominated by fluvial, alluvial fan, lacustrine and lake-delta facies of the Jogmaya Mandir, Fatehgarh, Barmer Hill, Dharvi Dungar and Thumbli Formations. These rocks are overlain by the Middle to Late Eocene post-rift continental facies of the Akli and Nagarka Formations, the latter recording the infilling of the rift basin topography.

Oligocene strata are absent in the Barmer Basin and the BMU erodes into the underlying Eocene rocks across much of the basin, although the intensity of erosion decreases southwards. Above the BMU, Miocene to Recent deposits of the Jagardia and Uttarlai Formations comprise continental alluvial deposits. Recent alluvium and stabilized aeolian dunes complete the basin fill.

3.3. The BMU in the Barmer Basin

3.3.1 Recognition and mapping of the BMU in the subsurface

In the seismic reflection data, the BMU within the Barmer Basin is imaged as a regional ~Middle Eocene to Early Miocene erosion surface. Due to erosion following regional southward tilting across a major structural hinge line that is one of the prominent Aravalli-trending basement ridges, the BMU is only preserved south of the Kaameshwari and Saraswati fields (Figure 4); the BMU deepens southwards, from only 600-700m beneath the subsurface in the Raageshwari Field to 1200m subsurface in the Guda area. The unconformity surface has been folded and cut by later fault reactivations around the basin (Figure 5). Within the central and southern regions of the Barmer Basin and southwards into the adjoining Sanchor sub-basin the BMU is identified using two- and three-dimensional seismic datasets supplemented by wireline well logs, cuttings and log correlations (Figure 6). Vertical seismic resolution is ~20 m within the Eocene-Miocene sequences.

In the northern part of the Barmer Basin, the younger regional uplift has resulted in erosion of progressively older stratigraphic units including the BMU (Figure 4). Consequently, the pre-erosion extent of the BMU across the northern part of the Barmer Basin remains speculative. However, projection of the uniform dip of the unconformity surface (~2°) northwards indicates a missing section of ≈ 1km above the northern outcrops. This is consistent with apatite fission track data which indicate that ~ 1 km of uplift and erosion have taken place in the northern part of the basin [*Dolson et al.*, 2015]. In comparison, the southern Barmer Basin underwent much less post-Oligocene erosion (typically <200 m) and preserves up to 250m of Nagarka Formation sediments, although individual fold structures (such as in the Guda Field area) indicate as much as ~300 m of inversion where the Nagarka Formation has been completely removed.

The BMU is represented in the seismic reflection data by a clear, bright, regionally correlatable reflector and evidence of scouring and channelling into the underlying sediments is seen on seismic sections (Figure 5). The lacustrine facies that make up the Eocene sequence below the BMU are recognized from the regionally extensive lignitic, sand-poor intervals separated by thick lacustrine shales [*Dolson et al.*, 2015].

Above the BMU, the continental facies of the Jagadia Formation is typically ~250 m in thickness [*Dolson et al.*, 2015]. The base of the Jagardia Formation is marked by a sudden influx of predominantly fine grained, carbonaceous sandstones and the formation is characterised by an upward increase in shale as depicted in the gamma-ray logs (Figure 6).

Wireline logs in representative wells (Figure 6) reveal the lithological contrast at the BMU. In the sonic log in particular, a distinct change to higher acoustic velocities is observed beneath the unconformity, since these sediments are typically more compacted and/or cemented compared to those above.

3.3.2 Dating the BMU

Whilst the majority of the Nagarka Formation, beneath the BMU, comprises lacustrine sediments, a brief but distinct shallow marine incursion deposited thin calcareous shales which provide good biostratigraphic control. *Bower et al.* [2004] (Supplementary Information 1) document the occurrence of *D. Barbadiensis* and *Cribrocentrum reticulatum,* indicating that the Nagarka Formation is aged between the base of calcareous nannofossil zone NP17 and top NP19/20 [*Agnini et al.*, 2014; *Wade et al.*, 2011]. The presence of *Helicosphaera lophota*, less commonly used as a range fossil, would restrict the upper age limit to NP18. Thus the Nagarka Formation ranges between ~40-35 Ma in age, i.e. Mid to Late Eocene. This is consistent with published work depicting a Bartonian-Priabonian [*Naidu et al.*, 2017] or Priabonian [*Compton*, 2009; *Dolson et al.*, 2015] age for this formation.

Above the unconformity in the Barmer Basin, the biofacies of the Jagardia Formation comprise an impoverished assemblage consisting of non-age diagnostic, long-ranging pollen species [Supplementary Information 1; *Bower et al.*, 2004]. However, in the Cambay Basin, where the Jagadia Formation is defined, the age of the Jagadia Formation is constrained by its locally conformable lower contact with the well-dated marine part of the Kand Formation, established to be of Lower-Mid Miocene (Burdigalian) age [*Chowdhary*, 2004]. The Jagadia Formation is thus considered to range from Middle to Upper Miocene in the Cambay Basin and the base of this formation is seismically correlated from the Cambay Basin through to the Barmer Basin (Figure 3).

Dolson et al. [2015] used vitrinite reflectance (VR) and apatite fission track analysis (AFTA) data to constrain the timing of erosion in the basin, which led to the formation of the BMU. *Naidu et al.* [2017] used the VR data of *Dolson et al.* [2015] to model exhumation as occurring from Late Oligocene through Pliocene with the most pronounced exhumation occurring between 26 Ma and 11 Ma, whilst noting that precise dating was difficult to define.

4. Causal mechanism for the base Miocene NW Indian plate intraplate basin unconformities

4.1. BMU development in the NW Indian intraplate basins associated with Himalayan tectonics?

Some previous research considered the formation of the BMU as related to Himalayan tectonics. *Compton* [2009] noted the similarity in age of the BMU in the Barmer Basin with an equivalent unconformity in the Jaisalmer Basin and related it to tectonics associated with the India-Asia collision (Fig. 3 in *Compton* [2009]). *Dolson et al.* [2015] also considered the Barmer Basin BMU to be the result of inversion related to the India-Asia collision. We consider this potential relationship further, below.

Rift basin inversion is common in orogenic forelands due to the compressive stress field [e.g. *Hansen and Nielsen*, 2003]. In general, basin inversion begins when the neighbouring orogenic zone has reached a sufficient elevation to impose significant forces on the foreland, and lasts until the end of mountain building. However, the return to deposition above the BMU in the NW Indian intraplate basins (Figure 1), in rocks that continue to be affected by the stress-field relating to the India-Asia collision, strongly suggests that this inversion is not responsible for the creation of the BMU in the NW Indian intraplate basins.

Regarding the possibility of formation of the BMU related to plate loading and flexure associated with he Himalayan orogeny, uplift in a flexural forebulge is also a frequently proposed mechanism to explain the occurrence of the Oligocene unconformity in the Himalayan peripheral foreland basin (e.g. DeCelles et al., 1998, DeCelles et al., 2004, Najman and Garzanti, 2000, Najman et al., 2005, Irfan et al., 2005, Bera et al., 2010). In the Himalayan peripheral foreland basin, a Late Eocene to Early Miocene unconformity has been consistently recorded along strike-length of the basin, from Pakistan, through India, to Nepal (Figure 1, panels 1-3). If passage through a flexural forebulge were the cause of all the unconformities in the northern Indian basins, the age of these unconformities would be expected to decrease away from the mountain range, as the more distal basins would have entered the forebulge region at a later time. The broadly synchronous age of the unconformities in the NW Indian

Intraplate basins, and those exposed in the uplifted peripheral foreland basin in the Himalaya, therefore implies that the basins do not share a common flexural origin. However, if the elastic thickness is large enough, flexural forebulges can be hundreds of kilometres wide (e.g. ~600 km for an elastic thickness of 75 km, see calculations below). It would therefore be possible to create a synchronous unconformity over a large area as a result of, for example, base-level fall superimposed on a wide flexural forebulge. Therefore, in order to test whether flexure could have played a role in the formation of the BMU in the NW Indian plate intraplate basins, including the Barmer Basin, we have undertaken plate reconstructions, flexural modelling, and a comparison with estimates of the elastic thickness in the region.

All flexural effects relating to mass changes in the proto-Himalaya (such as due to thickening or erosion) have a horizontal length-scale of effect that depends upon the elastic thickness of the Indian lithosphere. This length-scale arises because the elastic thickness of the lithosphere determines the distance between the orogenic load and the forebulge that flanks the foreland basin. Any cause of the unconformity related to flexural loading or unloading in the Himalaya and Tibetan Plateau therefore only operates over this length-scale. Here we test whether proposed causes of the unconformity relating to Himalayan tectonics, as outlined in the Introduction, are compatible with the location of the BMU in the NW Indian intraplate basins.

4.1.1. Plate reconstructions

We have used plate reconstructions to determine the distance between the NW Indian intraplate basins and the migrating Himalayan-Tibet deformation front during the Cenozoic. This is achieved by using the India-Somalia-NW Africa-North America-Eurasia plate circuit to calculate the distance between the Barmer Basin and stable Eurasia (based upon oceanic magnetic anomalies), and geological estimates of shortening in the India-Asia collision zone to infer the distance between stable Eurasia and the proto-Himalayan deformation front. We have calculated the maximum (i.e. southern Cambay Basin) and minimum (i.e. northern Barmer Basin) distances between the migrating deformation front and the BMU in the NW Indian intraplate basins. To calculate the location of the basins relative to stable Eurasia, we use the GPLATES software package [http://www.gplates.org *Boyden et al.*, 2011]. The reconstructions presented here use the India-Asia rotation poles of *Molnar and Stock* [2009] and Copley et al. [2010]. We infer the location of the proto-Himalayan deformation front relative to stable Eurasia using the estimate of 900 km of shortening within Asia since the India-Asia collision from *Van Hinsbergen et al.* [2011] and *Huang et al.* [2015]. As this value is difficult to determine, error bars of +/- 50% are used on this estimate. We assume that this shortening occurred at a steady rate since the collision, which we have taken to occur at the maximum and minimum generally accepted collision date values of ~60 Ma to by 50 Ma [*DeCelles et al.*, 2014; *Hu et al.*, 2015; *Najman et al.*, 2010; *Wang et al.*, 2011; *Wu et al.*, 2014]. By assuming that the shortening rate in Asia has been constant through time, we are likely to under-estimate the distance between the deformation front and the BMU in the NW Indian Intraplate basins, if the shortening rate actually decreased through time in tandem with the overall convergence rate (e.g. *Molnar and Stock* [2009]). By using a range of rotation poles, collision ages, and amounts of post-collision shortening within Asia, our models encompass a range of possible sizes of ‘greater India’. Our estimated variation through time of the distance between the BMU in the NW Indian intraplate basins and the deformation front is shown in Figure 7a. The calculated polygons include the range of distances produced by varying the parameters described above.

4.1.2. Flexural models

The Late Oligocene, ~ 26 Ma, is the time suggested by AFTA and VR data for the formation of the BMU in the Barmer Basin (see section 3.3.2). At this time, the northern Barmer and southern Cambay basins were located between ~1200 and ~2000 km from the palaeo-deformation front (Figure 7a). The range in this estimate represents the most extreme values calculated by varying the point of interest (i.e. northern Barmer or southern Cambay), the collision age, the rotation poles used, and the amount of post-collision shortening in Asia.

To test whether flexural effects could result in the formation of the BMU at the distances from the deformation front we have determined, a model is used for the flexure of an elastic plate overlying an inviscid half-space (see *Turcotte and Schubert* [2002] for a derivation of the relevant equations). We use a model for the loading of the lateral end of a plate by a vertical line load, and assume that there are no along-strike variations in the plate or load, so the model can be constructed along a 2-D plane perpendicular to the load (also known as a 'broken plate' model, and used as standard in this type of tectonic setting; *Turcotte and Schubert* [2002]). In this study we are concerned with the lateral position of the flexural forebulge, and not the amplitude, so the magnitude of the load plays no role in the analysis, as it has no effect on the length-scale of the deformation. The distance between the point of loading and the flexural forebulge, where surface uplift occurs, is shown in Figure 7b. Greater elastic thicknesses result in flexure over a longer wavelength and the formation of a forebulge at greater distances from the deformation front. Our calculations show that an elastic thickness of >110 km is required to form the BMU in the northern Barmer Basin by uplift of a flexural forebulge at ~26 Ma. An elastic thickness of >190 km is required for this effect to extend to the southern Cambay Basin.

Because of the uncertainties involved in using AFTA and VR data to estimate the date of erosion to form the BMU [*Naidu et al.*, 2017], we also perform calculations using the range of possible ages for the formation of the BMU based upon the palaeontological age constraints (see section 3.3.2). Using the youngest possible age for the erosion to form the BMU of 11 Ma (youngest possible age of the Kand Formation), the equivalent elastic thickness estimates are 70 km and 125 km. Using the oldest possible age of the Nagarka Formation (40 Ma), the estimates are 160 km and 325 km. Comparison of these values to estimates of the elastic thickness of the Indian plate allows us to establish whether a flexural mechanism for the formation of the BMU is plausible, as detailed below.

Numerous attempts have been made to constrain the elastic thickness of the Indian plate using the variation in gravity anomalies, or foreland basin depth, along profiles through the northern Indian subcontinent [e.g. *Bilham et al.*, 2003; *Karner and Watts*, 1983; *Lyon-Caen and Molnar*, 1985; *Maggi et al.*, 2000; *McKenzie and Fairhead*, 1997; *Watts and Burov*, 2003]. These studies obtained estimates of the elastic thickness ranging from <40 km to >100 km, with a poorly-constrained upper bound. *Jackson et al.* [2008] demonstrated that the choice of the location where the flexed plate is broken (i.e. the lateral end of the plate in the models, beneath the load, where a vertical load and bending moment are applied) has a strong control on the resulting estimate of the elastic thickness, for any method involving fitting gravity anomalies or basin geometries along profiles. In India, the location of the plate break is not known from observations, and if this parameter is not fixed in the inversions then a wide range of elastic thicknesses of greater then ~30 km can fit the data in northern India equally well. Furthermore, Craig and Copley [2014] demonstrated that the combination of the permanent deformation of the flexing plate due to foreland faulting, the unknown yield stress of the lithosphere, and uncertainties regarding the total force transmitted through the lithosphere, prevents the elastic thickness from being accurately estimated from profiles through forelands and oceanic outer rises.

An alternative approach to estimate the elastic thickness is to compare the topography and gravity anomalies in the frequency domain. The range of wavelengths over which these two quantities vary in tandem with each other is diagnostic of the elastic thickness of the region [*McKenzie and Bowin*, 1976; *Watts*, 2001]. Most frequency-domain estimates of elastic thicknesses have used the method of *Forsyth* [1985], which obtains the transfer function between the topography and the Bouguer gravity anomaly. However, *McKenzie* [2003] argued that in regions where topography has been removed by erosion, this method gives only an upper bound on the elastic thickness. *McKenzie et al.* [2014] proposed an alternative method, using recently collected satellite gravity data and the transfer function between the free-air gravity anomalies and the topography. They estimated that the elastic thickness in India is 25-32 km. This value is consistent with the estimates constructed using profiles through gravity anomalies or foreland basin depth, as described above, in cases where the 'plate break' is not artificially fixed in the inversions (*Jackson et al.* [2008]). Models using elastic thickness estimates in this range are also able to reproduce the observed width of the foreland basin, which is equivalent to the width of the negative gravity anomaly (*McKenzie and Fairhead*, 1997). For an elastic thickness of 25-32 km, the wavelength of the flexure is too short to have resulted in the formation of the BMU of the NW Indian intraplate basins in a flexural forebulge (Figure 7b).

4.2 The BMU caused by mantle circulation?

With the length-scale of flexural effects ruling out Himalayan tectonics as the cause of the BMU in the NW Indian Intraplate Basins, we must consider alternative mechanisms to explain the unconformity. We note the approximately coeval nature of the unconformity developed in the Himalayan peripheral foreland basin (Figure 1) and suggest that a single cause may explain both the BMU of the NW Indian Intraplate basins and the Oligocene unconformity in the Himalayan foreland basin, based on their temporal equivalence. We turn to potential causes that can explain unconformities over regional scales. We describe how sub-plate mantle circulation can produce the effects we observe. This circulation could be the result of slab-breakoff beneath the proto-Himalaya, or the ongoing background convection of the mantle, decoupled from shallow tectonics. Presently-available information does not allow us to distinguish between these potential causes, but either would represent the production of the BMU as a result of surface uplift due to mantle circulation.

We first examine the background convection of the mantle, unrelated to shallow tectonics. Upwelling in the convecting mantle can result in surface uplift of up to ~2 kilometres, over length-scales of up to tens of thousands of kilometres, but has also been observed to have effects on length-scales <1000 km and amplitudes of less than 500 m [e.g. *Hoggard et al.*, 2016; *Panasyuk and Hager*, 2000; *Winterbourne et al.*, 2014] For Rayleigh numbers (10^6-10^8; *McKenzie et al.* [1974]) that correspond to the Earth's mantle, numerical and laboratory experiments [e.g. *Larsen and Yuen*, 1997; *Schubert et al.*, 2001] suggest that transient temperature anomalies propagate through the convective system, and would be expected to produce transient vertical motions at the Earth's surface. Such uplift can result in shallow sedimentary basins and continental margins switching from deposition to erosion, on timescales of hundreds of thousands to tens of millions of years [*Burgess et al.*, 1997; *Jones et al.*, 2012; *Meyers et al.*, 1998; *Rudge et al.*, 2008]. A well-documented example of mantle dynamics affecting regional uplift is identified within the North Atlantic, where hot and buoyant material is advected beneath the plates from the Icelandic plume, resulting in a regional unconformity within the stratigraphic record of the Faeroe-Shetland and the Porcupine basins [e.g. *N White and Lovell*, 1997]. However, uplift and subsidence related to mantle circulation has been observed globally, not just near to large plumes [*Hoggard et al.*, 2016].

Alternatively, slab break-off related processes have been proposed to explain the Oligocene unconformity within the Himalayan peripheral foreland basin [e.g. *Husson et al.*, 2014; *Najman et al.*, 2004]. There are two aspects of this process that may cause uplift: the change in stresses being transmitted through the lithosphere, and the flow in the surrounding mantle induced by the sinking of the slab (which would cause subsidence) and its replacement by hot asthenosphere (which would lead to uplift). In the case of changing the stresses being transmitted through the lithosphere, the wavelength of deformation would be comparable to that relating to other forces affecting the flexure of the elastic Indian plate, and so incompatible with the results of this study. However, the large-scale mantle flow that can result from slab break-off can potentially affect much larger regions [e.g. *Husson et al.*, 2014]. In this case, the timing of break-off can be used to assess the likelihood that this event led to the arrival of hot, less dense mantle material causing uplift and thus a regional northern Indian unconformity. A range of ages have been proposed for slab break-off events in the India-Asia collision zone [*Webb et al.*, 2017], ranging from 45 Ma [*Replumaz et al.*, 2014] to 25 Ma [*Maheo et al.*, 2002], and as recent as 15 Ma [*Husson et al.*, 2014]. This range of suggested ages for slab break-off events are therefore compatible with the formation of the Oligocene unconformity in the peripheral foreland basin and the BMU in the NW Indian Intraplate basins, but a direct causal link is difficult to establish.

With the information we have available, it is therefore not possible to distinguish whether the BMU is directly related to slab break-off, or to the background high-Rayleigh-number convection in the mantle, but we conclude that sub-plate mantle circulation of some form is the likely cause. *Husson et al.* [2014] also suggested a role for mantle flow in the vertical motions of India and Tibet. Although there is little evidence for the kilometre-scale uplifts and depressions in the Indian plate suggested at the present day by their models, or the gravity anomalies that would be associated with such deflections, their work demonstrates the potential spatial extent and amplitude of vertical surface motions driven by convective circulation.

Our results highlight that correctly understanding the cause of unconformity surfaces requires carefully mapping and correlating their full extent, and their potential continuations into adjacent basins. The question then becomes what controls the extent of such surfaces. The radically different expression of the BMU in terms of the time-interval of missing sediments in the various

NW Indian Intraplate Basins shows that the local depositional environment (e.g. basin depth, continental or marine sedimentation) can play an important role in controlling whether an unconformity is formed, as well as its extent and erosional intensity. This effect limits our ability to know whether the lessening of the BMU southwards corresponds to decreasing amounts of uplift, or to more pre-uplift accommodation space reducing the effects of the vertical motions. To resolve this question, palaeo-water-depth estimates are required. The combination of these effects means that in regions commonly thought to be dominated by the effects of local tectonics, the correct interpretation of unconformity surfaces requires regional-scale mapping of multiple basins, otherwise the potential over-printing effects of mantle circulation could be misinterpreted.

5. Conclusions

The sedimentary successions of the NW Indian Plate Intraplate Basins are punctuated by a major Late Eocene-Early Miocene unconformity called the Base Miocene Unconformity (BMU). We show that the NW Indian intraplate Barmer Basin unconformity is unrelated to Himalayan tectonics. The resumption of deposition post-unconformity rules out inversion due to compression associated with India-Asia convergence as a cause, as these compressive forces are still present. The large distance between the NW Indian Plate Intraplate Basins and the Himalayan front excludes flexural effects. The coeval nature of the Himalayan peripheral foreland basin and NW Indian Plate Intraplate Basin unconformities may suggest a common cause. We propose that the unconformity within the Himalayan peripheral foreland basin and NW Indian Plate Intraplate Basins may be a result of mantle circulation, either due to subducting slab break-off or high-Rayleigh-number background convection. Our results suggest that such circulation can produce geological signatures even in regions where collisional tectonics may be expected to dominate, and suggests that the interpretation of unconformities rests strongly on mapping out their full extent, and coeval structures in adjacent basins.

Acknowledgements

Marie Skłodowska-Curie Actions and the iTECC (Investigating Tectonism-Erosion-Climate-Couplings) EU ITN FP7 research network funded this research under grant agreement 316966. Cairn India Limited kindly provided seismic datasets, well data and access to internal reports for determining the extent of the BMU within the Barmer Basin, and to whom further requests for access should be directed. They, along with JV partners ONGC, are thanked for granting permission to publish these data. Our appreciation is extended to various members of the subsurface team at Cairn India Limited for helpful discussions during the research whilst the interpretation of regional data and ideas developed through discussions with members of the Basin Dynamics Group at Keele University. Paul Bown from UCL is thanked for providing his expertise to our understanding of the biostratigraphic data. This paper benefitted from careful and thorough reviews from Peter Clift and Peter DeCelles.

FIGURE CAPTIONS

Figure 1. Stratigraphic summary columns of key reference sections of the Himalayan peripheral foreland basin (Panels 1-4) and NW Indian Plate Intraplate Basins (5-9) highlighting the presence of the ~late Oligocene to early Miocene (BMU) unconformity. Inset map shows the location of the stratigraphic panels. JM= Jogdia Mandir Formation, Dh=Dhandlawas Formation. H numbers refer to the regionally mapped erosional events in the Bombay Basin [*Chowdhary*, 1975; *Chowdhary and Singh*, 1978; *Kundal et al.*, 2005]. The NW Indian Plate Intraplate Basins (panels 1-4) are described and referenced extensively in the text. Considering the peripheral Himalayan foreland basin: furthest west, in the Kohat and Potwar Plateaus of Pakistan (panel 1), Miocene continental facies of the Rawalpindi Group (Murree and overlying Kamlial Formations) unconformably overlie Eocene marine facies of various formation names. In the Kohat Plateau, the youngest marine facies are the Kohat Formation of Middle Eocene age, [*Pivnik and Wells*, 1996], and rocks of similar age are recorded to the east in the Potwar plateau [*Shah*, 2009]. The Murree Formation of the uppermost Rawalpindi Group is considered to be of Early Miocene age, based on mammal fossil evidence [*Shah*, 2009]. In the Potwar Plateau, the base of the Rawalpindi Group overlying the Eocene rocks is magnetostratigraphically dated at 18 Ma [*Johnson et al.*, 1985]. In northern India (panel 2), the top of the marine Subathu Formation is dated biostratigraphically as Lutetian [*Batra*, 1989; *Mathur*, 1978].The overlying continental red beds are called the Dagshai or Dharamsala Formation, depending on location. Best dated is the Dharamsala Formation, which magnetostratigraphic analysis constrains to date from 20 Ma, with the lowest 250 m being undatable by magnetostratigraphy due to lack of continuity of the section [*N M White et al.*, 2002]. Maximum depositional ages provided by Ar-Ar dates of detrital white mica support the magnetostratigraphic dating, with modal mica ages at the base of the measured section of 22-24 Ma. Micas dated in samples from the thin unit below the magnetostratigraphic section yield similar Ar-Ar ages. The age of the Dagshai Formation has only been constrained using detrital minerals to provide a maximum depositional age, with

an age of <31 Ma suggested for the base of the section by zircon fission track analysis [*Najman et al.*, 2004] and <25 Ma and <22 Ma from detrital mica Ar-Ar ages from samples within the unit [*Najman et al.*, 1997]. In Nepal (panel 3), the upper part of the marine Bhainskati Formation underlying the unconformity is considered to be of Middle to Late Eocene age in Central Nepal [*Sakai*, 1989], whilst Late Paleocene to Early Eocene fossils are reported in West Nepal [*Fuchs and Frank*, 1970]. Above the unconformity, the base of the red beds of the Dumre Formation are dated at 20 Ma by magnetostratigraphy [*Ojha et al.*, 2008], consistent with the maximum age of the formation dated at <19 Ma from detrital Ar-Ar dating of white micas [*DeCelles et al.*, 2001].

Figure 2. Outline sketch map of the main sedimentary basins of northwest India and southern-central Pakistan. White areas denote where basement is either at or very close to surface. Thrust lines in the Sulaiman and Kirthar fold belts are indicative.

Figure 3. North-South oriented seismic section showing correlation of the BMU through the Barmer, Sanchor and Cambay Basins. Colour bar on top right of figure indicates seismic amplitudes from low (blue) to high (yellow). The BMU reflector is highlighted in yellow. Inset shows location of seismic line in the Barmer Basin, which can be located in Figure 2. Red overlay indicates the interpreted presence of basement as penetrated in the Deodar-1 well in the Patan Basin in the northern part of the Cambay Basin.

Figure 4. (**A**) Map of the base Miocene unconformity (BMU) surface coloured for true vertical depth (TVD) in metres as determined from seismic and well data sets. (**B**) Map of the extensional fault network in the Barmer Basin displayed on the pre-rift (base Cretaceous) unconformity horizon. The grey shaded areas represent the hade of the faults, showing the horizontal displacement between footwall and hanging wall. The location and extent of the BMU

surface is shown by the bold solid line, which is equivalent to the region shown in (A). Straight black lines show the extent of the merged 3D seismic grid and selected regional 2D lines. (**C**) Locations of wells referred to in the text displayed on the same fault map as in (B).

Figure 5. High-resolution grey-scale dip seismic lines through representative W-E cross-sections of the BMU showing surface features. Location of the seismic lines are shown in right hand insets and in Figure 4. Abbreviated horizons TDD = Top Dharvi Dungar; IDD = Intra-Dharvi Dungar; TBH = Top Barmer Hill. (**A**) The BMU is present as a bright, gently undulose reflector across the Barmer Basin, highlighted in green, locally cut by reactivated faults that extend from deeper in the section. The base of the BMU is clearly erosional and an alluvial wedge progrades across the normal fault in the centre of the section. Truncation of older sediments under the BMU is clearly visible. Wells with GR profile shown tied to the BMU surface. (**B**) Example of the BMU surface cut by post-BMU fault activity within the central Barmer Basin. Note the strong truncation surfaces beneath the BMU. Left without interpretation, right with picked horizons.

Figure 6. Summary wireline and lithogical logs of the Nagarka and Jagadia formations, allowing identification of the BMU in representative wells along a north-south transect across the southern Barmer Basin. Note the presence of ~10 m thick, stacked, sharp-based sandstones in the Jagadia Formation and an overall sonic ‘slowness’ of this formation. By contrast, the Nagarka Formation is dominated by coals and coaly shales with only thin sandstones and siltstones being developed. GR is the gamma ray log measured in API units from 0 clean sandstone to 150 units radioactive shale. Sonic log shows the interval transit time (Δt) of the rocks, the inverse of velocity, measured in microseconds per foot. The higher sonic velocities

reflect greater burial and compaction of the sediments beneath the BMU. Wells located on Fig 4. Numbers give depth in metres.

Figure 7: (a) The distance between the north Barmer (pale grey) and south Cambay (dark grey) basins and the migrating Himalayan deformation front. Shaded polygons define the range of possible distances, calculated by varying the age of collision, the amount of post-collision shortening within Asia, and the rotation poles used. (b) The pale grey polygon shows the distance between a load and the near and far margins of the associated flexural forebulge, as a function of the elastic thickness of the flexing plate. Horizontal shaded regions show the possible distances between the Himalayan front and the N Barmer and S Cambay basins at 26 Ma (when the BMU is likely to have formed), taken from the calculations shown in (a). The horizontal dashed lines show the smallest possible distances, at the youngest possible age of the unconformity (11 Ma).

SUPPLEMENTARY INFORMATION

Supplementary Information 1: biostratigraphic data used to data the BMU [*Bower et al.*, 2004]

References

Agnini, C., E. Fornaciari, I. Raf, R. Catanazariti, H. Pälike, J. Backman, and D. Rio (2014), Biozonation and biochronology of Paleogene calcareous nannofossils from low and middle latitudes, *Newsletters on Stratigraphy*, *47*, 131-181.

Basu, D., A. Banerjee, and D. Tamhane (1982), Facies distribution and petroleum geology of the Bombay offshore basin, India, *Journal of Petroleum Geology*, *5*(1), 51-75.

Batra, R. S. (1989), A Reinterpretation of the Geology and Biostratigraphy of the Lower Tertiary Formations Exposed Along the Bilaspur-Shimla Highway, Himachal-Pradesh, India, *Journal of the Geological Society of India*, *33*(6), 503-523.

Bera, M., A. Sarkar, P. Chakraborty, V. Ravikant, and A. Choudhury (2010), Forced regressive shoreface sandstone from Himalayan foreland: implications to early Himalayan tectonic evolution, *Sedimentary Geology*, *229*(4), 268-281.

Bhandari, L., and L. Chowdhary (1975), Stratigraphic Analysis of Kadi and Kalol Formations, Cambay Basin, India, *AAPG Bulletin*, *59*(5), 856-871.

Bhandari, L., and S. Jain (1984), Reservoir geology and its rle in the development of the L-III resrvoir, Bombay High field, India., *Journal of Petroleum Geology*, *7*(1), 27-46.

Bilham, R., R. Bendick, and K. Wallace (2003), Flexure of the Indian plate and intraplate earthquakes, *Journal of Earth System Science*, *112*(3), 315-329.

Biswas, S. (1987), Regional tectonic framework, structure and evolution of the western marginal basins of India, *Tectonophysics*, *135*(4), 307-327.

Bladon, A. J., S. M. Clarke, and S. D. Burley (2015a), Complex rift geometries resulting from inheritance of pre-existing structures: Insights and regional implications from the Barmer Basin rift, *Journal of Structural Geology*, *71*, 136-154.

Bladon, A. J., S. D. Burley, S. M. Clarke, and H. Beaumont (2015b), Geology and regional significance of the Sarnoo Hills, eastern rift margin of the Barmer Basin, NW India, *Basin Research*, *27*(5), 636-655.

Bower, S., J. Brady, R. Hodgkinson, and J. Boucher (2004), Stratigraphic Framework for the Barmer Basin, Rajasthan, *Cairn Energy Technical Report ED/RJ-ON-90/1/GEO/01/03/1428*.

Boyden, J. A., R. D. Müller, M. Gurnis, T. H. Torsvik, J. A. Clark, M. Turner, H. Ivey-Law, R. J. Watson, and J. S. Cannon (2011), Next-generation plate-tectonic reconstructions using GPlates.

Burgess, P. M., M. Gurnis, and L. Moresi (1997), Formation of sequences in the cratonic interior of North America by interaction between mantle, eustatic, and stratigraphic processes, *Geological Society of America Bulletin*, *109*, 1515-1535.

Calvès, G., A. M. Schwab, M. Huuse, P. D. Clift, C. Gaina, D. Jolley, A. R. Tabrez, and A. Inam (2011), Seismic volcanostratigraphy of the western Indian rifted margin: The pre-Deccan igneous province, *Journal of Geophysical Research: Solid Earth*, *116*(B1).

Carmichael, S., S. Akhter, J. Bennett, M. Fatimi, K. Hosein, R. Jones, M. Longacre, M. Osborne, and R. Tozer (2009), Geology and hydrocarbon potential of the offshore Indus Basin, Pakistan, *Petroleum Geoscience*, *15*(2), 107-116.

Chowdhary, L. (1975), Reversal of basement-block motions in Cambay basin, India, and its importance in petroleum exploration, *AAPG Bulletin*, *59*(1), 85-96.

Chowdhary, L. (2004), *Petroleum Geology of the Cambay Basin, Gujarat., India*, Indian Petroleum Publishers.

Chowdhary, L., and L. Singh (1978), Early Eocene subaerial erosional valleys in Cambay Basin, India, *AAPG Bulletin*, *62*(3), 442-454.

Clift, P. D., and S. VanLaningham (2010), A climatic trigger for a major Oligo-Miocene unconformity in the Himalayan foreland basin, *Tectonics*, *29*(5).

Clift, P. D., N. Shimizu, G. D. Layne, J. S. Blusztajn, C. Gaedicke, H. U. Schluter, M. K. Clark, and S. Amjad (2001), Development of the Indus Fan and its significance for the erosional history of the Western Himalaya and Karakoram, *Geological Society of America Bulletin*, *113*(8), 1039-1051.

Coblentz, D. D., M. Sandiford, R. M. Richardson, S. H. Zhou, and R. Hillis (1995), The origins of the intraplate stress-field in continental Australia, *Earth and Planetary Science Letters*, *133*(3-4), 299-309.

Compton, P. M. (2009), The geology of the Barmer Basin, Rajasthan, India, and the origins of its major oil reservoir, the Fatehgarh Formation, *Petroleum Geoscience*, *15*(2), 117-130.

Copley, A., J. P. Avouac, and J. Y. Royer (2010), India-Asia collision and the Cenozoic slowdown of the Indian plate: Implications for the forces driving plate motions, *Journal of Geophysical Research-Solid Earth*, *115*.

Copley, A., S. Mitra, R. A. Sloan, S. Gaonkar, and K. Reynolds (2014), Active faulting in apparently stable peninsular India: Rift inversion and a Holocene-age great earthquake on the Tapti Fault., *Journal of Geophysical Research Solid Earth*, *119*, doi:10.1002/2014JB011294.

Craig, T. J., and A. Copley (2014), An explanation for the age independence of oceanic elastic thickness estimates from flexural profiles at subduction zones, and implications for continental rheology, *Earth and Plametary Science Letters*, *392*, 207-216.

Craig, T. J., J. Jackson, K. Priestley, and D. McKenzie (2011), Earthquake distribution patterns in Africa: their relationship to variations in lithospheric and geological structure, and their rheological implications, *Geophysical Journal International*, *185*(1), 403-434.

Cunningham, D. (2005), Active intracontinental transpressional mountain building in the Mongolian Altai: Defining a new class of orogen, *Earth and Planetary Science Letters*, *240*(2), 436-444.

DeCelles, P. G. (2012), Foreland Basin Systems Revisited: Variations in Response to Tectonic Settings, in *Tectonics of Sedimentary Basins*, edited by C. Busby and A. A. Pérez, pp. 405-426, John Wiley & Sons, Ltd.

DeCelles, P. G., G. E. Gehrels, J. Quade, and T. P. Ojha (1998), Eocene early Miocene foreland basin development and the history of Himalayan thrusting, western and central Nepal, *Tectonics*, *17*(5), 741-765.

DeCelles, P. G., P. Kapp, G. E. Gehrels, and L. Ding (2014), Paleocene-Eocene foreland basin evolution in the Himalaya of southern Tibet and Nepal: Implications for the age of initial India-Asia collision, *Tectonics*, *33*(5), 824-849.

DeCelles, P. G., G. E. Gehrels, Y. Najman, A. J. Martin, and E. Garzanti (2004), Detrital geochronology and geochemistry of Cretaceous-Early Miocene strata of Nepal: Implications for timing and diachroneity of initial Himalayan orogenesis., *Earth and Planetary Science Letters*, *227*, 313-330.

DeCelles, P. G., D. M. Robinson, J. Quade, T. P. Ojha, C. N. Garzione, P. Copeland, and B. N. Upreti (2001), Stratigraphy, structure, and tectonic evolution of the Himalayan fold-thrust belt in western Nepal, *Tectonics*, *20*(4), 487-509.

Dezes, P., S. M. Schmid, and P. A. Ziegler (2004), Evolution of the European Cenozoic Rift System: interaction of the Alpine and Pyrenean orogens with their foreland lithosphere, *Tectonophysics*, *389*, 1-33.

Dhir, R., and A. Singhvi (2012), The Thar Desert and its antiquity, *Current Science*, 1001-1008.

Dickinson, W. R., and W. S. Snyder (1978), Plate tectonics of the Laramide Orogeny, *Memoirs of the GEological Society of America*, *151*, doi: 10.1130/MEM1151-p1355.

Dolson, J., S. D. Burley, V. Sunder, V. Kothari, B. Naidu, N. P. Whiteley, P. Farrimond, A. Taylor, N. Direen, and B. Ananthakrishnan (2015), The discovery of the Barmer Basin, Rajasthan, India, and its petroleum geology, *AAPG Bulletin*, *99*(3), 433-465.
Forsyth, D. W. (1985), Subsurface loading and estimates of the flexural rigidity of continental lithosphere, *Journal of Geophysical Research: Solid Earth*, *90*(B14), 12623-12632.
Fuchs, G., and W. Frank (1970), Geological investigations in west Nepal and their significance for the geology of the Himalayas., *Geologische Rundschau*, *59*, 552-580.
Hansen, D. L., and S. B. Nielsen (2003), Why rifts invert in compression, *Tectonophysics*, *373*(1), 5-24.
Hoggard, M. J., N. M. White, and D. Al-Attar (2016), Global dynamic topography observations reveal limited influence of large-scale mantle flow., *Nature Geoscience*, *9*, 456-463.
Hu, X., E. Garzanti, T. Moore, and I. Raffi (2015), Direct stratigraphic dating of India-Asia collision onset at the Selandian (middle Paleocene, 59±1 Ma), *Geology*, *43*(10), 859-862.
Huang, W., D. J. Hinsbergen, P. C. Lippert, Z. Guo, and G. Dupont-Nivet (2015), Paleomagnetic tests of tectonic reconstructions of the India-Asia collision zone, *Geophysical Research Letters*, *42*(8), 2642-2649.
Huggett, J., S. Burley, F. Longstaffe, S. Saha, and M. Oates (2015), The Nature and Origin of Authigenic Chlorite and Related Cements in Oligo–Miocene Reservoir Sandstones, Tapti Gas Fields, Surat Depression, Offshore Western India, *Journal of Petroleum Geology*, *38*(4), 383-409.
Husson, L., M. Bernet, S. Guillot, P. Huyghe, J.-L. Mugnier, A. Replumaz, X. Robert, and P. Van der Beek (2014), Dynamic ups and downs of the Himalaya, *Geology*, *42*(10), 839-842.
Irfan, M., M. Shahid, M. Haroon, and N. Zadi (2005), Sargodha high: a flexure forebuldge of the himalayan foreland basin, *Geological Bulletin, University of Peshawar*, *38*, 149-156.
Jackson, J., D. McKENZIE, K. Priestley, and B. Emmerson (2008), New views on the structure and rheology of the lithosphere, *Journal of the Geological Society*, *165*(2), 453-465.
Johnson, N. M., J. Stix, L. Tauxe, P. F. Cerveny, and R. A. K. Tahirkheli (1985), Paleomagnetic Chronology, Fluvial Processes, and Tectonic Implications of the Siwalik Deposits near Chinji Village, Pakistan, *Journal of Geology*, *93*(1), 27-40.
Jones, S. M., B. Lovell, and A. G. Crosby (2012), Comparison of modern and geological observations of dynamic support from mantle convection, *Journal of the Geological Society*, *169*(6), 745-758.
Kaila, K., H. Tewari, V. Krishna, M. Dixit, D. Sarkar, and M. Reddy (1990), Deep seismic sounding studies in the north Cambay and Sanchor basins, India, *Geophysical Journal International*, *103*(3), 621-637.
Karner, G., and A. Watts (1983), Gravity anomalies and flexure of the lithosphere at mountain ranges, *Journal of Geophysical Research: Solid Earth*, *88*(B12), 10449-10477.
Krishna, K. S., J. M. Bull, and R. A. Scrutton (2009), Early (pre-8 Ma) fault activity and temporal strain accumulation in the central Indian Ocean, *Geology*, *37*, 227-230.
Kundal, P., S. Mude, and S. K. Humane (2005), Ichnofossils from the Late Eocene to Early Miocene of Narmada Block of Cambay Basine, Gujarat, India, *Jour. of the Porbandar area, Saurashtra Gujarat, India. Jour. Palaeontol. Soc. India*, *50*(2), 177-182.
Larsen, T. B., and D. A. Yuen (1997), Ultrafast upwelling bursting through the upper mantle, *Earth and Planetary Science Letters*, *146*(3-4), 393-399.
Lyon-Caen, H., and P. Molnar (1985), Gravity-Anomalies, Flexure of the Indian Plate, and the Structure, Support and Evolution of the Himalaya and Ganga Basin, *Tectonics*, *4*(6), 513-538.

Lyon-Caen, H., and P. Molnar (1985), Gravity anomalies, flexure of the Indian plate, and the structure, support and evolution of the Himalaya and Ganga Basin, *Tectonics*, *4*(6), 513-538.

Maggi, A., J. Jackson, D. Mckenzie, and K. Priestley (2000), Earthquake focal depths, effective elastic thickness, and the strength of the continental lithosphere, *Geology*, *28*(6), 495-498.

Maheo, G., S. Guillot, J. Blichert-Toft, Y. Rolland, and A. Pecher (2002), A slab breakoff model for the Neogene thermal evolution of South Karakoram and south Tibet, *Earth and Planetary Science Letters*, *195*, 45-58.

Mathur, N. S. (1978), Biostratigraphical aspects of the Subathu Formation, Kumaun Himalaya., *Recent Researches in Geology*, *5*, 96-112.

Mathuria, T., A. Julka, P. Dimri, and P. Pandey (2011), Hydrocarbon Prospectivity in Stratigraphic Traps within Cambay Shale, Broach Sub Block, Cambay Basin, India, *Search and Discovery Article*, *10326*.

McKenzie, D. (2003), Estimating Te in the presence of internal loads, *Journal of Geophysical Research: Solid Earth*, *108*(B9).

McKenzie, D., and C. Bowin (1976), The relationship between bathymetry and gravity in the Atlantic Ocean, *Journal of Geophysical Research*, *81*(11), 1903-1915.

McKenzie, D., and D. Fairhead (1997), Estimates of the effective elastic thickness of the continental lithosphere from Bouguer and free air gravity anomalies., *Journal of Geophysical Research*, *102*, 523-527.

McKenzie, D., J. M. Roberts, and N. O. Weiss (1974), Convection in the Earth's mantle: towards a numerical simulation, *Journal of Fluid Mechanics*, *62*(3), 465-538.

McKenzie, D., W. Yi, and R. Rummel (2014), Estimates of T-e from GOCE data., *Earth and Planetary Science Letters*, *399*, 116-127.

Mehrotra, N. C., B. Venkatachala, and P. Kapoor (2010), Palynology in hydrocarbon exploration: High impact palynological studies in Western Offshore and Krishna-Godavari Basin, *Journal of the Geological Society of India*, *75*(2), 364-377.

Meyers, J. B., B. R. Rosendahl, C. G. A. Harrison, and Z.-D. Ding (1998), Deep-imaging and gravity results from the offshore Cameroon Volcanic Line, and speculation of African hotlines, *Tectonophysics*, *284*, 31-61.

Mohan, M. (1995), Cambay basin-a promise of oil and gas potential, *Journal of the Palaeontological Society of India*, *40*, 41-47.

Mohan, R., S. N. Tewari, and S. Mayor (2008), Evidence of multiple phases of basin inversion in the Narmada Block, South Cambay Basin, Gujarat, India, paper presented at 7th International Conference on Petroleum Geophysics.

Molnar, P., and J. M. Stock (2009), Slowing of India's convergence with Eurasia since 20 Ma and its implications for Tibetan mantle dynamics, *Tectonics*, *28*(3).

Müller, R. D., V. Yatheesh, and M. Shuhail (2015), The tectonic stress field evolution of India since the Oligocene, *Gondwana Research*, *28*(2), 612-624.

Naidu, B. S., S. Burley, J. Dolson, P. Farrimond, V. Sunder, V. Kothari, P. Mohapatra, and N. Whiteley (2017), Hydrocarbon generation and migration modelling in the Barmer Basin of western Rajasthan, India: lessons for exploration in rift basins with late stage inversion, uplift and tilting, Petroleum System Case Studies, v, edited, Memoir.

Najman, Y., and E. Garzanti (2000), Reconstructing early Himalayan tectonic evolution and paleogeography from Tertiary foreland basin sedimentary rocks, northern India, *Geological Society of America Bulletin*, *112*(3), 435-449.

Najman, Y., K. Johnson, N. White, and G. Oliver (2004), Evolution of the Himalayan foreland basin, NW India, *Basin Research*, *16*(1), 1-24.

Najman, Y., A. Carter, G. Oliver, and E. Garzanti (2005), Provenance of Eocene foreland basin sediments, Nepal: Constraints to the timing and diachroneity of early Himalayan orogenesis, *Geology*, *33*(4), 309-312.

Najman, Y., M. S. Pringle, M. R. W. Johnson, A. H. F. Robertson, and J. R. Wijbrans (1997), Laser Ar-40/Ar-39 dating of single detrital muscovite grains from early foreland-basin sedimentary deposits in India: Implications for early Himalayan evolution, *Geology*, *25*(6), 535-538.

Najman, Y., E. Appel, M. Boudagher-Fadel, P. Bown, A. Carter, E. Garzanti, L. Godin, J. Han, U. Liebke, and G. Oliver (2010), Timing of India-Asia collision: Geological, biostratigraphic, and palaeomagnetic constraints, *Journal of Geophysical Research: Solid Earth*, *115*(B12).

Ojha, T., R. Butler, P. G. DeCelles, and J. Quade (2008), Magnetic polarity stratigraphy of the Neogene foreland basin deposits of Nepal, *Basin Research*, *doi: 10.1111/j.1365-2117.2008.00374.x*.

Otto, S. C. (1997), Mesozoic-Cenozoic history of deformation and petroleum systems in sedimentary basins of Central Asia; implications of collisions on the Eurasian margin, *Petroleum Geoscience*, *3*(4), 327-341.

Panasyuk, S. V., and B. H. Hager (2000), Models of isostatic and dynamic topography, geoid anomalies, and their uncertainties, *Journal of Geophysical Research*, *105*, 28,199-128,209.

Pangtey, K. (1996), Positive inversion structures and the possibility of strike-slip movement in the Tapti-Daman sub-basin, *Bulletin of the Oil and Natural Gas Corporation*, *33*, 91-112.

Pivnik, D. A., and N. A. Wells (1996), The transition from Tethys to the Himalaya as recorded in northwest Pakistan, *Geological Society of America Bulletin*, *108*(10), 1295-1313.

Quadri, V.-u.-n., and S. Shuaib (1986), Hydrocarbon prospects of southern Indus basin, Pakistan, *The American Association of Petroleum Geologists Bulletin*, *70*(6), 730-747.

Replumaz, A., and P. Tapponnier (2003), Reconstruction of the deformed collision zone between India and Asia by backward motion of lithospheric blocks, *Journal of Geophysical Research-Solid Earth*, *108*(B6).

Replumaz, A., F. Capitanio, S. Guillot, A. Negredo, and A. Villaseñor (2014), The coupling of Indian subduction and Asian continental tectonics, *Gondwana Research*, *26*(2), 608-626.

Rudge, J. F., M. E. S. Champion, N. M. White, D. McKenzie, and B. Lovell (2008), A plume model of transient diachronous uplift at the Earth's surface, *Earth and Planetary Science Letters*, *267*(1), 146-160.

Sahoo, T. R., and M. Choudhuri (2011), Tectono-Sedimentary Evolution of Northern part of Cambay Basin.

Sakai, H. (1989), Rifting of Gondwanaland and uplifting of the Himalayas recorded in Mesozoic and Tertiary fluvial sediments in the Nepal Himalayas., in *Sedimentary Facies in the Active Plate Margin.*, edited by A. Taira , Masuda, F., pp. 723-732, Terra Scientific Publishing Company, Tokyo.

Sanyal, S., L. Wood, D. Chatterjee, N. Dwivedi, and S. Burley (2012), A high resolution sequence stratigraphic approach to correlate complex sub-seismic tidally influenced estuarine incised valley fill reservoirs of the Lakshmi Field, Gulf of Cambay, India, paper presented at Gulf of Cambay, India: 2012 International Conference and Exhibition, AAPG, Extended Abstracts.

Schubert, G., D. L. Turcotte, and P. Olson (2001), *Mantle convection in the Earth and planets*, Cambridge University Press.
Shah, I. (2009), Stratigraphy of Pakistan., *Memoirs of the Geological Survey of Pakistan*, *22*, 381.
Sharma, K. K. (2007), K-T magmatism and basin tectonism in western Rajasthan, India, results from extensional tectonics and not from Réunion plume activity., *in Foulger, G.R., and Jurdy, D.M., eds., Plates, plumes, and planetary processes: Geological Society of America Special Paper*, *430*, 775-784.
Siddiquie, H. (1963), The jodhpur-malani divide separating the Barmer and Jaisalmer basins, *Geological Society of India*, *4*, 97-108.
Singh, A., C. Singh, and B. Kennett (2015), A review of crust and upper mantle structure beneath the Indian subcontinent, *Tectonophysics*, *644*, 1-21.
Turcotte, D. L., and G. Schubert (2002), *Geodynamics*, Second ed., Cambridge University Press.
Valdiya, K. (1976), Himalayan transverse faults and folds and their parallelism with subsurface structures of north Indian plains, *Tectonophysics*, *32*(3-4), 353357359377379-353357355375386.
Van Hinsbergen, D. J., P. Kapp, G. Dupont-Nivet, P. C. Lippert, P. G. DeCelles, and T. H. Torsvik (2011), Restoration of Cenozoic deformation in Asia and the size of Greater India, *Tectonics*, *30*(5).
Wade, B. S., P. N. Pearson, W. A. Berggren, and H. Palike (2011), Review and revision of Cenozoic tropical planktonic foraminiferal biostratigraphy and calibration to the geomagnetic polarity and astronomical time scale., *Earth Science Reviews*, *104*, 111-142.
Wandrey, C. J. (2004), *Bombay geologic province Eocene to Miocene composite total petroleum system, India*, US Department of the Interior, US Geological Survey.
Wandrey, C. J., B. Law, and H. A. Shah (2004), *Sembar Goru/Ghazij composite total petroleum system, Indus and Sulaiman-Kirthar geologic provinces, Pakistan and India*, US Department of the Interior, US Geological Survey.
Wang, J., X. Hu, L. Jansa, and Z. Huang (2011), Provenance of the Upper Cretaceous–Eocene deep-water sandstones in Sangdanlin, southern Tibet: Constraints on the timing of initial India-Asia collision, *The Journal of Geology*, *119*(3), 293-309.
Watts, A. B. (2001), *Isostasy and Flexure of the Lithosphere*, Cambridge University Press.
Watts, A. B., and E. Burov (2003), Lithospheric strength and its relationship to the elastic and seismogenic layer thickness, *Earth and Planetary Science Letters*, *213*(1), 113-131.
Webb, A. A. G., H. C. Guo, P. D. Clift, L. Husson, T. Muller, D. Costantino, A. Yin, Z. Q. Xu, H. Cao, and Q. Wang (2017), The Himalaya in 3D: Slab dynamics controlled mountain building and monsoon intensification, *Lithosphere*, *9*(4), 637-651.
White, N. and B. Lovell (1997), Measuring the pulse of a plume with the sedimentary record, *Nature*, *387*(6636), 888-891.
White, N. M., M. Pringle, E. Garzanti, M. Bickle, Y. Najman, H. Chapman, and P. Friend (2002), Constraints on the exhumation and erosion of the High Himalayan Slab, NW India, from foreland basin deposits, *Earth and Planetary Science Letters*, *195*(1-2), 29-44.
Winterbourne, J., N. White, and A. Crosby (2014), Accurate measurements of residual topography from the oceanic realm, *Tectonics*, *33*(6), 982-1015.
Wu, F.-Y., W.-Q. Ji, J.-G. Wang, C.-Z. Liu, S.-L. Chung, and P. D. Clift (2014), Zircon U–Pb and Hf isotopic constraints on the onset time of India-Asia collision, *American Journal of Science*, *314*(2), 548-579.

Fig 1.

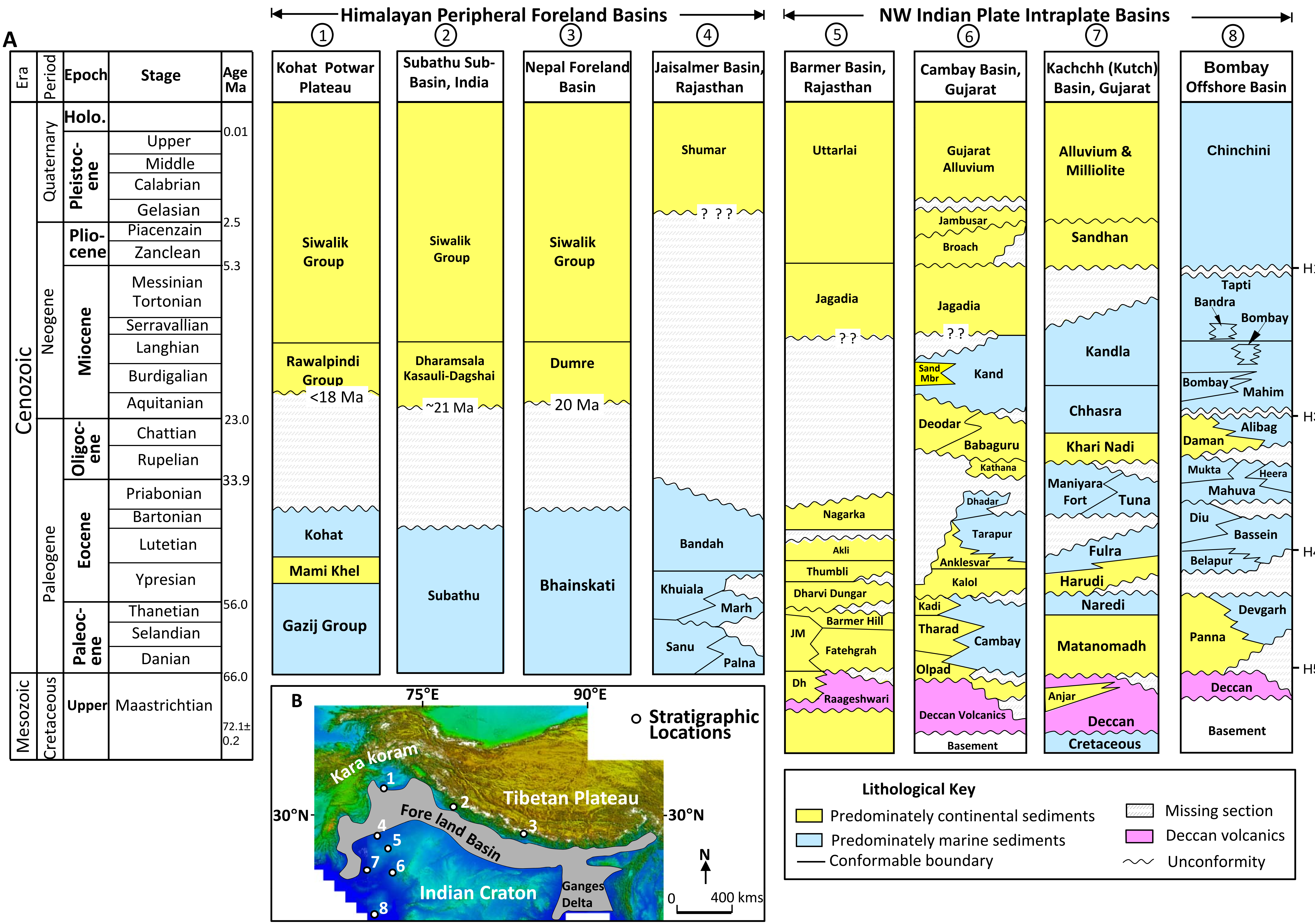

Himalayan Peripheral Foreland Basins
NW Indian Plate Intraplate Basins
A
Era
Period
Epoch
Stage
Age Ma
Cenozoic
Mesozoic
Quaternary
Neogene
Paleogene
Cretaceous
Holo.
Pleistoc-ene
Plio-cene
Miocene
Oligoc-ene
Eocene
Paleoc-ene
Upper
Upper
Middle
Calabrian
Gelasian
Piacenzain
Zanclean
Messinian
Tortonian
Serravallian
Langhian
Burdigalian
Aquitanian
Chattian
Rupelian
Priabonian
Bartonian
Lutetian
Ypresian
Thanetian
Selandian
Danian
Maastrichtian
0.01
2.5
5.3
23.0
33.9
56.0
66.0
72.1±0.2
1
Kohat Potwar Plateau
Siwalik Group
Rawalpindi Group
<18 Ma
Kohat
Mami Khel
Gazij Group
2
Subathu Sub-Basin, India
Siwalik Group
Dharamsala Kasauli-Dagshai
~21 Ma
Subathu
3
Nepal Foreland Basin
Siwalik Group
Dumre
20 Ma
Bhainskati
4
Jaisalmer Basin, Rajasthan
Shumar
? ??
Bandah
Khuiala
Marh
Sanu
Palna
5
Barmer Basin, Rajasthan
Uttarlai
Jagadia
??
Nagarka
Akli
Thumbli
Dharvi Dungar
Barmer Hill
JM
Fatehgrah
Dh
Raageshwari
6
Cambay Basin, Gujarat
Gujarat Alluvium
Jambusar
Broach
Jagadia
??
Sand Mbr
Kand
Deodar
Babaguru
Kathana
Dhadar
Tarapur
Anklesvar
Kalol
Kadi
Tharad
Cambay
Olpad
Deccan Volcanics
Basement
7
Kachchh (Kutch) Basin, Gujarat
Alluvium & Milliolite
Sandhan
Kandla
Chhasra
Khari Nadi
Maniyara Fort
Tuna
Fulra
Harudi
Naredi
Matanomadh
Anjar
Deccan
Cretaceous
8
Bombay Offshore Basin
Chinchini
Tapti
Bandra
Bombay
Bombay
Mahim
Alibag
Daman
Mukta
Heera
Mahuva
Diu
Bassein
Belapur
Devgarh
Panna
Deccan
Basement
H1
H3
H4
H5
B
75°E
90°E
30°N
30°N
Stratigraphic Locations
Kara koram
Tibetan Plateau
Fore land Basin
Indian Craton
Ganges Delta
1
2
3
4
5
6
7
8
N
0
400 kms
Lithological Key
Predominately continental sediments
Predominately marine sediments
Conformable boundary
Missing section
Deccan volcanics
Unconformity

Fig 2.

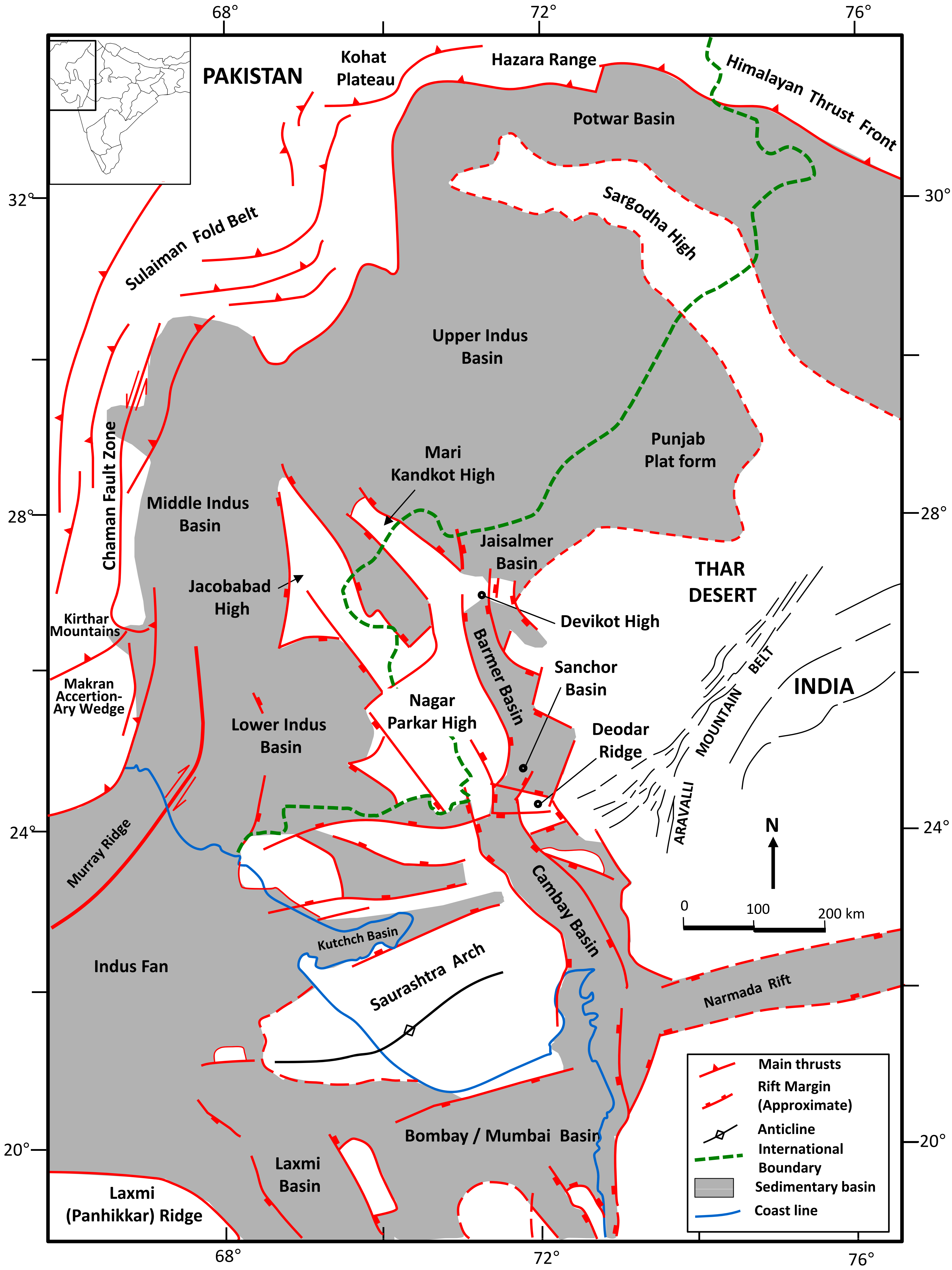
68°
72°
76°
32°
30°
28°
24°
20°
PAKISTAN
Kohat Plateau
Hazara Range
Himalayan Thrust Front
Potwar Basin
Sargodha High
Sulaiman Fold Belt
Upper Indus Basin
Punjab Plat form
Mari Kandkot High
Chaman Fault Zone
Middle Indus Basin
Jaisalmer Basin
THAR DESERT
Jacobabad High
Devikot High
Kirthar Mountains
Barmer Basin
Sanchor Basin
Makran Accertion-Ary Wedge
Nagar Parkar High
Lower Indus Basin
Deodar Ridge
INDIA
ARAVALLI MOUNTAIN BELT
N
Murray Ridge
Cambay Basin
0
100
200 km
Kutchch Basin
Indus Fan
Saurashtra Arch
Narmada Rift
Main thrusts
Rift Margin (Approximate)
Anticline
International Boundary
Sedimentary basin
Coast line
Bombay / Mumbai Basin
Laxmi Basin
Laxmi (Panhikkar) Ridge

Fig 3.

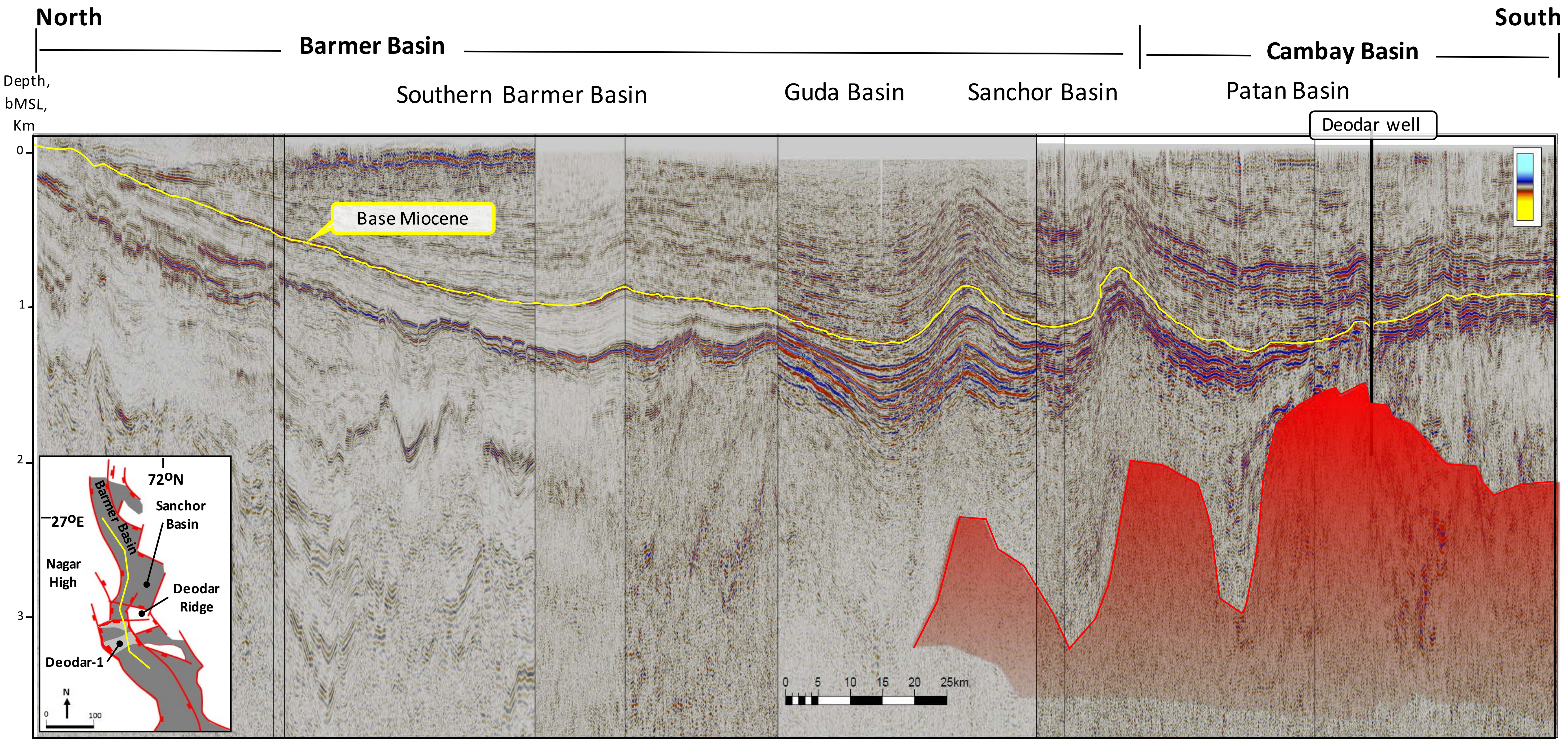

North
South
Barmer Basin
Cambay Basin
Depth, bMSL, Km
Southern Barmer Basin
Guda Basin
Sanchor Basin
Patan Basin
Deodar well
Base Miocene
0
1
2
3
0 5 10 15 20 25km
72ºN
27ºE
Barmer Basin
Sanchor Basin
Nagar High
Deodar Ridge
Deodar-1
N
0 100

Fig 4.

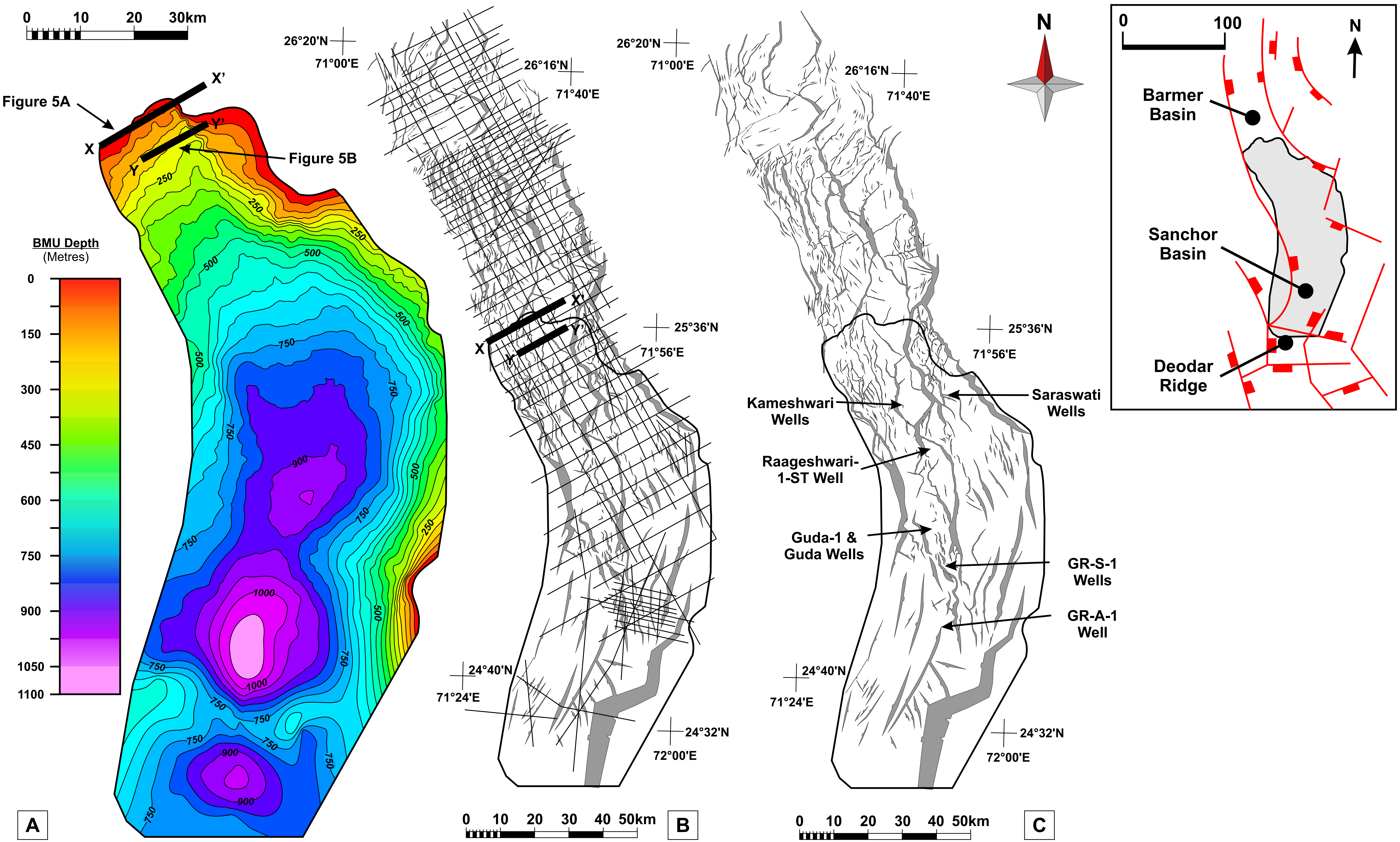

0 10 20 30km
Figure 5A
X
X'
Y
Y'
Figure 5B
BMU Depth
(Metres)
0
150
300
450
600
750
900
1050
1100
250
500
750
900
1000
A
26°20'N
71°00'E
26°16'N
71°40'E
25°36'N
71°56'E
24°40'N
71°24'E
24°32'N
72°00'E
0 10 20 30 40 50km
B
Kameshwari Wells
Raageshwari-1-ST Well
Guda-1 & Guda Wells
Saraswati Wells
GR-S-1 Wells
GR-A-1 Well
C
N
0 100
Barmer Basin
Sanchor Basin
Deodar Ridge

Fig 5.

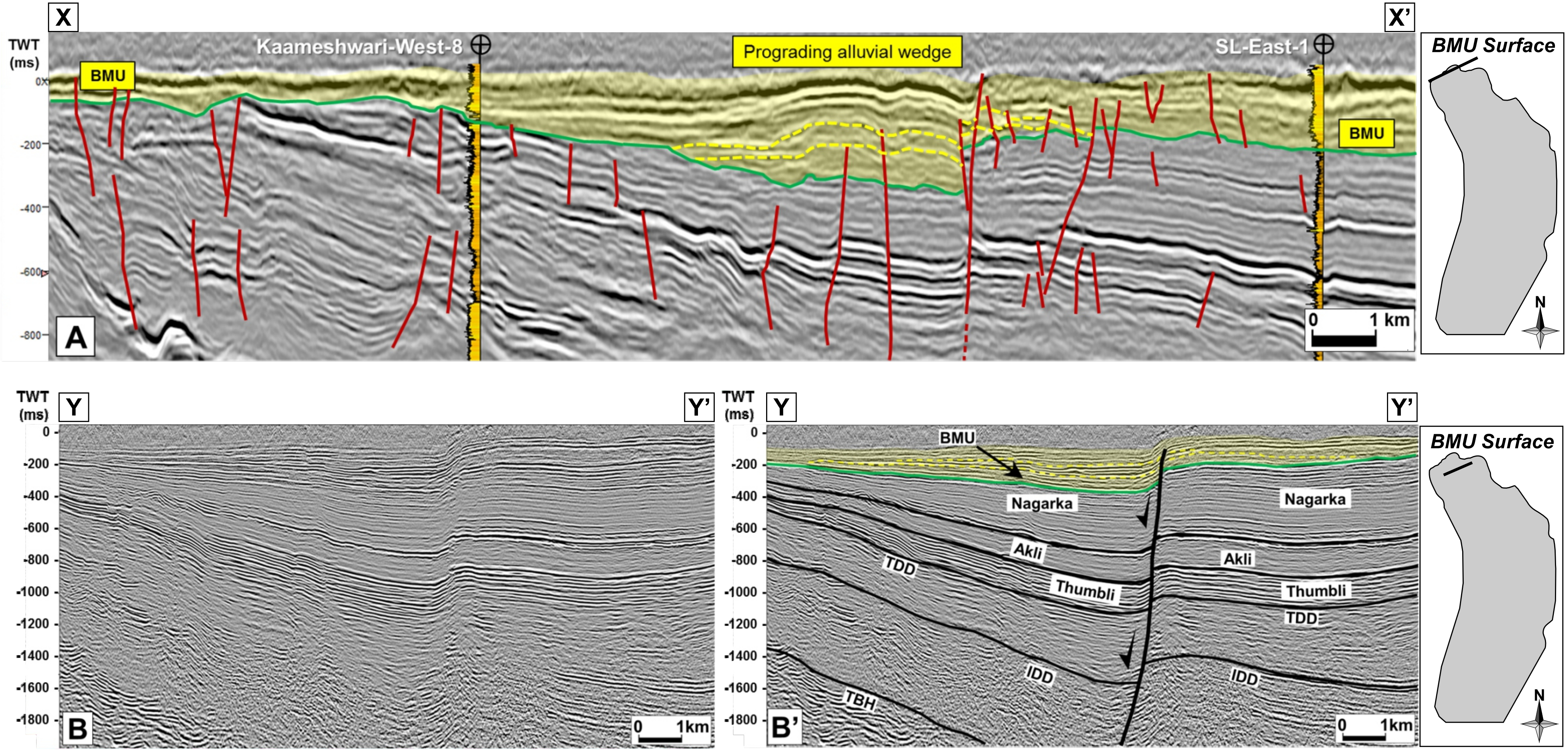

X
X'
TWT (ms)
Kaameshwari-West-8
Prograding alluvial wedge
SL-East-1
BMU
BMU
BMU Surface
N
0 1 km
A
Y
Y'
TWT (ms)
0
-200
-400
-600
-800
-1000
-1200
-1400
-1600
-1800
B
0 1km
B'
BMU
Nagarka
Nagarka
Akli
Akli
Thumbli
Thumbli
TDD
TDD
IDD
IDD
TBH
BMU Surface
N

Fig 6.

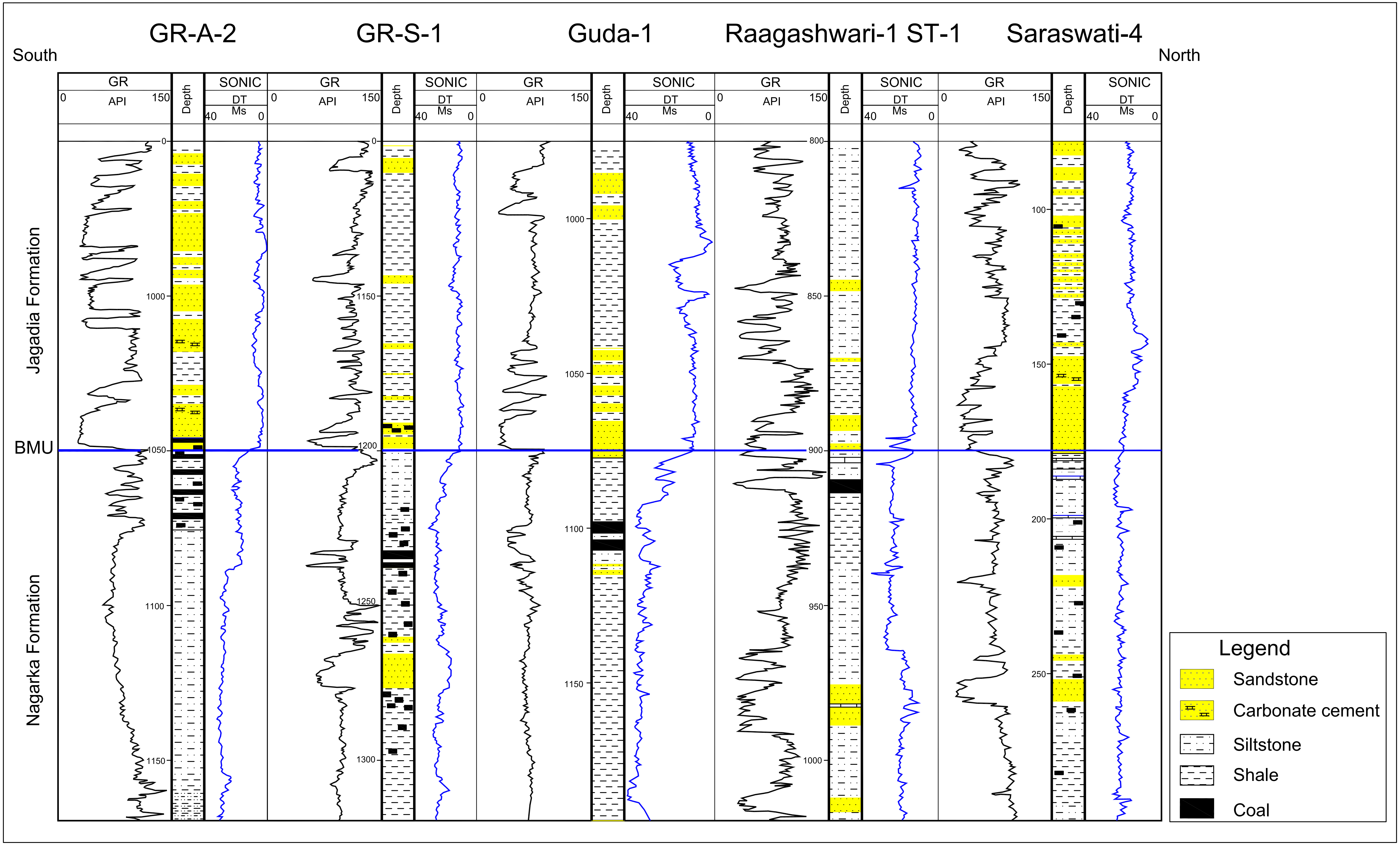

GR-A-2
GR-S-1
Guda-1
Raagashwari-1 ST-1
Saraswati-4
South
North
GR
API
0
150
Depth
SONIC
DT
Ms
40
0
Jagadia Formation
Nagarka Formation
BMU
Legend
Sandstone
Carbonate cement
Siltstone
Shale
Coal

Fig 7.

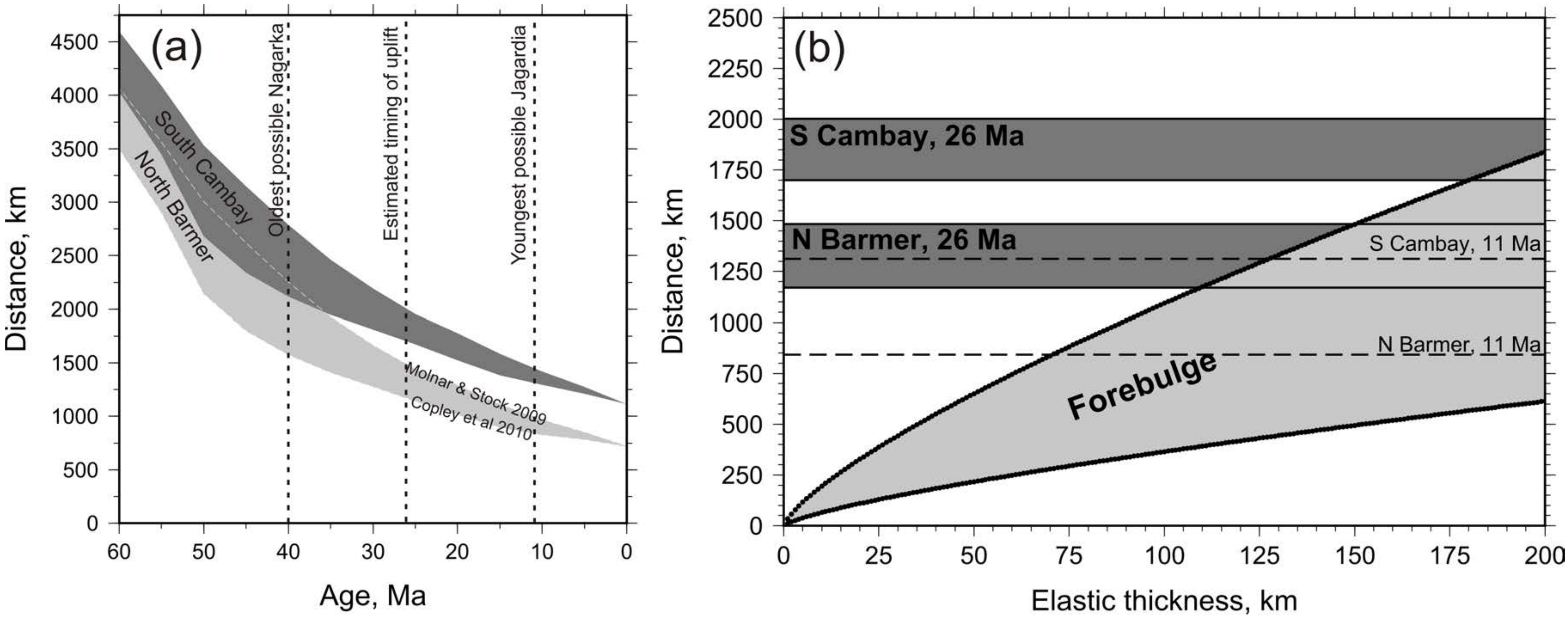

(a)
Distance, km
Age, Ma
South Cambay
North Barmer
Oldest possible Nagarka
Estimated timing of uplift
Youngest possible Jagardia
Molnar & Stock 2009
Copley et al 2010
(b)
Distance, km
Elastic thickness, km
S Cambay, 26 Ma
N Barmer, 26 Ma
S Cambay, 11 Ma
N Barmer, 11 Ma
Forebulge